HHS Public Access

Author manuscript

Neurobiol Dis. Author manuscript; available in PMC 2017 May 01.

Published in final edited form as:

Neurobiol Dis. 2016 May ; 89: 23–35. doi:10.1016/j.nbd.2016.01.013.

Dentate cannabinoid-sensitive interneurons undergo unique and selective strengthening of mutual synaptic inhibition in experimental epilepsy

Jiandong Yu[1,2], **Bogumila Swietek**[2,*], **Archana Proddutur**[2,*], and **Vijayalakshmi Santhakumar**[2]

[1]Guangdong-Hongkong-Macau Institute of CNS Regeneration, Jinan University, Guangzhou 510632, PR China

[2]Department of Pharmacology, Physiology and Neuroscience, Rutgers New Jersey Medical School, Newark, New Jersey 07103, USA

Abstract

Altered inhibition is a salient feature of hippocampal network reorganization in epilepsy. Hippocampal pyramidal cells and dentate granule cells show specific reduction in cannabinoid receptor type 1 (CB_1R)-sensitive GABAergic inputs in experimental epilepsy. In the dentate gyrus, CB_1Rs regulate synaptic release from accommodating interneurons (AC-INs) with adapting firing characteristics and axonal projections in the molecular layer, but not from fast-spiking basket cells (FS-BCs). However, it is not known whether the intrinsic physiology and synaptic inhibition of AC-INs responsible for CB_1R-sensitive inhibition is altered in epilepsy. Using the pilocarpine-induced status epilepticus (SE) model of epilepsy, we find that the basic physiological characteristics of AC-INs in epileptic rats are not different from age-matched controls. In paired interneuronal recordings, the amplitude of unitary inhibitory synaptic currents (uIPSCs) between AC-INs doubled after SE. Non-stationary noise analysis revealed that the post-SE strengthening of synapses between AC-INs resulted from an increase in postsynaptic receptors. Baseline synaptic release and CB_1R antagonist enhancement of release at synapses between AC-INs were not different between control and post-SE rats. Additionally, uIPSC amplitude in FS-BCs to AC-INs pairs was unchanged after SE indicating input-specific microcircuit alterations in inhibitory inputs to AC-INs. At the network level, AC-INs showed no reduction in spontaneous and miniature inhibitory synaptic current (sIPSC or mIPSC) frequency or amplitude after SE. However, AC-IN mIPSC amplitude was persistently enhanced in post-SE and epileptic rats. CB_1R agonist reduced the amplitude and suppressed a greater proportion of sIPSCs in AC-INs from post-SE and

Correspondence: Vijayalakshmi Santhakumar, PhD, Department of Pharmacology, Physiology and Neuroscience, Rutgers New Jersey Medical School, MSB-H-512, 185 S. Orange Ave. Newark, NJ 07103, santhavi@njms.rutgers.edu.

*Equal Contribution

Author contributions: J.Y., B.S., and A.P. performed experiments; J.Y. and B.S. analyzed data; J.Y., A.P., and V.S. interpreted results of experiments; J.Y., and A.P. prepared figures; J.Y. and V.S. conception and design of research; J.Y. A.P. and V.S. drafted manuscript.

epileptic rats demonstrating a novel, cell-type specific increase in CB_1R-sensitive inhibition of AC-INs after SE. This unique post-SE strengthening of inhibition between AC-INs could lead to activity-dependent suppression of AC-IN firing and compromise dentate CB_1R-sensitive inhibition in epilepsy.

Keywords

Epilepsy; seizure; interneuron; GABA; cannabinoid; dentate gyrus

Introduction

Epileptic circuits undergo profound changes in inhibitory regulation of projection neurons (Coulter, 1999; Zhang et al., 2007). Recent studies have identified that granule cell and CA1 pyramidal neurons from epileptic rodents show a selective decrease in a subset of inhibitory inputs that are modulated by cannabinoid type 1 receptors (CB_1R) (Wyeth et al., 2010; Sun et al., 2014). Similarly, we have demonstrated a functional decrease in CB_1R-sensitive inhibition of dentate fast-spiking basket cells (FS-BCs) in epileptic rats (Yu et al., 2015b). In the dentate gyrus, CB_1R-sensitive inhibition is mediated by two morphologically distinct GABAergic neurons: Hilar commissural-associational pathway-associated (HICAP-) cells with axons in the inner molecular layer and total molecular layer (TML-) cells with axons spanning the inner to outer molecular layers (Han et al., 1993; Soriano and Frotscher, 1993; Mott et al., 1997; Yu et al., 2015a). HICAP cells are known to express cholecystokinin (CCK) and CB_1R (Hefft and Jonas, 2005; Morozov et al., 2009; Savanthrapadian et al., 2014). In the cortex and hippocampus, CB_1R at axon terminals of CCK-positive neurons mediate a unique form of activity-dependent suppression of GABA release at synapses on projection neurons and CCK-expressing neurons alike (Ohno-Shosaku et al., 2001; Freund, 2003; Ali, 2007; Neu et al., 2007; Lee et al., 2010). Recently we demonstrated that TML neurons express CB_1R and show modulation of baseline GABA release by cannabinoid ligands (Yu et al., 2015a). HICAP and TML cells have comparable intrinsic and synaptic physiology, including accommodating firing and asynchronous release, and can be classified as a functionally similar class of accommodating interneurons (AC-INs) that mediate dentate CB_1R-sensitive inhibition (Yu et al., 2015b; Yu et al., 2015a). Previous studies have demonstrated that dentate inhibitory neurons can be lost or structurally and functionally altered after status epilepticus (SE) (Buckmaster and Jongen-Relo, 1999; Zhang and Buckmaster, 2009; Yu et al., 2013; Sun et al., 2014). However, whether the intrinsic and synaptic physiology of AC-INs, which underlies dentate CB_1R-sensitive inhibition, is altered in epilepsy has not been examined.

Identifying how the microcircuit that underlies CB_1R-sensitive inhibition is modified in epilepsy is essential, since drugs targeting CB_1Rs have been suggested as candidate anticonvulsant and anti-epileptogenic agents (Wallace et al., 2003; Echegoyen et al., 2009; Devinsky et al., 2014). While cannabinoid agonists reduce the duration of chemically induced seizures in naïve animals (Marsicano et al., 2003; Monory et al., 2006), they fail to limit seizure duration in epileptic animals (Wallace et al., 2003) demonstrating that CB_1R ligands act differently in naïve and epileptic circuits. Interestingly, CB_1R agonist reduces

occurrence of spontaneous seizures in epileptic animals (Wallace et al., 2003) indicating a role for CB_1R-dependent circuit actions in maintaining the balance between excitation and inhibition in epileptic circuits. In order to understand how inhibitory networks underlying dentate CB_1R-sensitive inhibition are altered after status epilepticus, we examined whether AC-IN intrinsic physiology and microcircuit interactions are modified in epilepsy.

Materials and Methods

Animals

All experiments were performed in accordance with Rutgers-NJMS, Newark, NJ, Institutional Animal Care and Use Committee (IACUC). Postnatal day 25–27, male, Wistar rats were pre-treated with scopolamine methyl nitrate (1 mg/kg, s.c) followed by pilocarpine (300 mg/kg, i.p) to induce stage 3 or greater seizures (Racine scale) (Yu et al., 2013). Use of male rats avoids confounds due to sex differences in inhibition and endocannabinoid signaling (Maguire and Mody, 2007; Craft et al., 2013). Diazepam (10 mg/kg, i.p.) was administered after 60 min of stage 3 or greater seizures. Control rats received saline (i.p.) after scopolamine treatment, followed by diazepam after 2 hours. A group of pilocarpine and saline treated rats were implanted with prefabricated surface recording electrodes (Pinnacle Technologies, Lawrence, KS) 19–35 days after SE and underwent continuous video-EEG monitoring 8h/day for 3 days. In our hands, 11 of 12 (91.67%) rats recorded between 25–45 days post-SE showed spontaneous electrographic seizures (defined as high amplitude activity, at least 2.5 times the standard deviation of the baseline) accompanied by simultaneous behavioral seizures (≥Racine stage 3). Therefore, rats over >40 days post-SE rats were deemed epileptic (Yu et al., 2015b). Recordings in the “epileptic” group in the current study included both rats with confirmed spontaneous seizures on video-EEG monitoring and rats >40 day post-SE that were presumed epileptic.

Physiology

One week (6–8 days) and 40–70 days after SE or saline treatment, rats were euthanized under isoflurane anesthesia. Horizontal brain slices (300 μM) were prepared in ice-cold oxygenated sucrose artificial CSF (sucrose-aCSF) containing (in mM): 75 sucrose, 85 NaCl, 25 D-glucose, 24 NaHCO3, 4 MgCl2, 2.5 KCl, 1.25 NaH2PO4, and 0.5 CaCl2, incubated at 32±1°C for 30 min in a submerged chamber containing 50% sucrose-aCSF and 50% recording aCSF (containing in mM: 126 NaCl, 26 NaHCO3, 10 D-glucose, 2.5 KCl, 2 CaCl2, 2 MgCl2 and 1.25 NaH2PO4 with 95% O2 and 5% CO2 at 7.4 pH) and held at room temperature (Gupta et al., 2012; Yu et al., 2013; Li et al., 2014). Interneurons at the border of the hilus and granule cell layer were visualized and patched under IR-DIC visualization using a Nikon Eclipse FN-1 microscope (40X water-immersion objective). Recordings were obtained at 32–33°C using borosilicate microelectrodes (3–4 MΩ) containing (in mM) 70 KCl, 70 K-gluconate, 10 HEPES, 2 MgCl2, 0.2 EGTA, 2 Na-ATP, 0.5 Na-GTP, 10 phosphocreatine and 0.2% biocytin. Neurons were initially held at −70 mV to determine responses to 1.5 sec positive and negative current injections for cell identification. Neurons with adapting firing without stuttering, and high input resistance (>150 MΩ) were considered AC-INs (Yu et al., 2015b). Cells with non-adapting, high frequency firing, and low input resistance (<150 MΩ) were classified as FS-BCs (Proddutur et al., 2013; Yu et al.,

2015a). Spike frequency adaptation was measured as the ratio of the first to last interspike interval ($ISI_{first/last}$ ratio) during a +500 pA current injection (Gupta et al., 2012). Sag ratio was calculated as the ratio between the steady-state and peak negative voltage responses to a −100 pA current injection. Post-hoc biocytin immunostaining and morphological analysis were used to definitively identify AC-INs based on dendrites in the hilus and molecular layer and axonal projections predominantly in the inner molecular layer or distributed across the total molecular layer (Harney and Jones, 2002; Zhang and Buckmaster, 2009; Hosp et al., 2014; Yu et al., 2015b; Yu et al., 2015a). FS-BCs had axon terminals in the granule cell layer. Neurons that showed fusiform or multipolar somata and those with spiny dendrites restricted to the hilus, were presumed to be hilar-perforant pathway-associated (HIPP) or mossy cells and were excluded from analysis. AC-INs, in which complete axonal arbors could not be recovered, were identified based on physiology, dendritic morphology (aspiny dendrites not restricted to the hilus) and/or immunoreactivity for CB_1R. Whole-cell voltage- and current-clamp recordings were obtained using Axon Instruments MultiClamp 700B (Molecular Devices, Sunnyvale, CA).

Signals were low-pass filtered at 3 kHz and digitized using DigiData 1440A at 10-kHz sampling frequency and acquired using pCLAMP (Molecular Devices). For paired recordings, the presynaptic interneuron was held in current-clamp and stimulated by 2–8 current pulses (3 ms, 700–1100pA) at 50 Hz every 10 s while the postsynaptic interneuron was recorded under voltage-clamp at −70 mV. For spontaneous and miniature inhibitory postsynaptic current (IPSC) recordings, interneurons were recorded in voltage-clamp (−70 mV) in the presence of kynurenic acid (3 mM) with series resistance compensation. Series resistance in voltage clamp recordings was < 20 MΩ and recordings were discontinued if series resistance increased by >20%. All salts and kynurenic acid were from Sigma and SCH 50911, (RS)-baclofen, WIN 55212-2 and AM251 were from Tocris Bioscience. WIN 55212-2 and AM251 stock solutions were made in dimethylsulfoxide (DMSO) and diluted before the experiment and the final DMSO concentration was not more than 0.1%.

Anatomy

Recorded slices were fixed in 0.1 M phosphate buffer containing 4% paraformaldehyde at 4°C for 2 days. For post-hoc immunohistochemistry, thick slices (300 μm) were incubated overnight at room temperature with anti-PV (PV-28, 1.5:1000, polyclonal rabbit, Swant) or anti-CB_1R antibody (1:1000, polyclonal guinea pig from Frontier Science, Hokkaido, Japan) in 0.3% Triton X-100 and 3% normal goat serum containing PBS. A subset of slices was re-sectioned at 50 μm and immunostained with rabbit anti-CCK antibody (1:2000, a gift from Dr. Akos Kulik, University of Freiburg, Germany). Immunoreactions were revealed using Alexa 488-conjugated secondary goat antibodies against rabbit IgG (1:500), and biocytin staining was revealed using Alexa 594-conjugated streptavidin (1:1000). Sections were visualized and imaged using a Nikon A1R laser confocal microscope with a 1.2 NA 60X water objective. Cell reconstructions and morphological analyses were performed with Neurolucida V.10.02 (MBF Bioscience, Williston, VT) using confocal image stacks (Gupta et al., 2012; Yu et al., 2015a).

Analysis

Spontaneous inhibitory synaptic currents (sIPSCs) and miniature inhibitory synaptic currents (mIPSCs) were analyzed using Clampfit (Molecular Devices, Sunnyvale, CA). sIPSCs were detected using event detection in Clampfit. Evoked IPSCs were measured using cursors. The latencies of uIPSCs were measured from peak of presynaptic action potentials to onset of IPSCs. Asynchronous release was quantified as the charge transfer in the duration 15 ms after the 8^{th} action potential in a train of 8 stimuli at 50 Hz until the return to baseline. Cumulative probability plots of sIPSC parameters were constructed by pooling an equal number of sIPSCs from each cell and compared using Kolmogorov-Smirnov (K-S) test (SigmaPlot 12.3, San Jose, CA).

Non-stationary variance analysis (Sigworth, 1980) was performed on unitary current responses from paired recordings between AC-INs to determine the peak conductance of synaptic $GABA_A$ channels. To isolate fluctuations in the current decay attributable to stochastic channel gating, the mean waveform was scaled to the peak of individual IPSCs (Traynelis et al., 1993; De Koninck and Mody, 1994). Successful responses were used to calculate the ensemble mean current (I) and peak-scaled variance (σ_{PS}^2) for each data point. Plots of variance versus current were fit with the equation: $\sigma_{PS}^2 = iI\ (I^2/N_P) + \sigma_B^2$, where i is the weighted-mean single-channel current, N_P is the number of channels open at peak synaptic current, and σ_B^2 is the background variance (Brickley et al., 1999). Only IPSCs that showed stable peak amplitude over time were included in the analysis. Paired and unpaired two-tailed Student's *t*-test (Microsoft Excel 2007, Redmond, WA) and Chi-Square test ($\chi 2$-test) were used to compare data, as appropriate. Mann-Whitney U test was used to compare data that failed the normality test (SigmaPlot 12.3, San Jose, CA). Significance was set to $p < 0.05$. Data are shown as mean ± s.e.m or median and interquartile range (IQR) as appropriate.

Results

AC-IN intrinsic physiology is not altered after SE

Dentate AC-INs included hilar neurons with both hilar and molecular layer dendrites, TML cells with axons in the inner, middle and outer molecular layers (Fig. 1A), and HICAP-like cells with axons in the commissural-associational pathway (Fig. 1B). Both TML and HICAP cells showed axonal expression of CB_1R (Fig. 1A–B). On the basis of their prominent spike frequency adaptation (Fig. 1C–D) and similar intrinsic physiology including firing frequency, resting membrane potential, input resistance (R_{in}) (Yu et al., 2015b), TML and HICAP cells responsible for dentate CB_1-sensitive inhibition were classified as AC-INs. Recorded neurons were processed for post-hoc morphological identification. AC-INs were distinguished from FS-BCs based on physiological and morphological characteristics as reported previously (Yu et al., 2015b; Yu et al., 2015a). Hilar neurons with stuttering firing and spiny dendrites confined to the hilus (Zhang et al., 2009; Hosp et al., 2014; Li et al., 2014; Savanthrapadian et al., 2014), likely to be HIPP cells, were not analyzed.

Dentate CB_1R-containing GABAergic neurons have been shown to undergo progressive structural reorganization during epileptogenesis (Karlocai et al., 2011). As reported earlier

(Yu et al., 2015b), AC-IN firing frequency and input resistance are not altered one week after pilocarpine-SE, in the early phase of epileptogenesis (Fig. 1E). The resting membrane potential (RMP in mV, control: −64.1±1.4, n=25; post-SE: −67.0±1.7, n=20, $p>0.05$ by *t*-test) and $ISI_{first/last}$ ratio ($ISI_{first/last}$, control: 0.29±0.02, n=25 cells; post-SE: 0.33±0.03, n=13 cells, $p>0.05$ by *t*-test) were also not altered in post-SE rats. Since SE can lead to progressive changes in cellular and network physiology, we examined presumed epileptic rats (which included both rats with spontaneous seizures on video-EEG monitoring and rats >40 days post-SE which were not examined for spontaneous seizures) for changes in AC-IN intrinsic physiology. As with post-SE rats, firing rate (Fig. 1F, frequency in Hz at 800 pA current injection, control: 59.1±6.2, n=12 cells, epileptic: 56.0±7.3, n=9 cells, $p>0.05$ by *t*-test) and $ISI_{first/last}$ ratio (not shown) were not different in AC-INs from epileptic and age-matched saline-injected control rats. Similarly, epileptic rats showed no changes in AC-IN resting membrane potential (RMP in mV, control: −57.5±1.5, n=12; epileptic: −55.1±2.7, n=7, $p>0.05$ by *t*-test) and R_{in} (R_{in} in MΩ, control: 234.5±12.8, n=12 cells, epileptic: 210.8±18.9, n=9 cells, $p>0.05$ by *t*-test). Thus, the basic firing and passive characteristics of AC-INs are not altered in post-SE and epileptic rats.

Strengthening of synapses between AC-INs after status epilepticus

Our recent studies demonstrated a cell-type specific post-SE decrease in the probability of synaptic release from AC-INs to FS-BCs (Yu et al., 2015b). To determine if synapses between AC-INs are compromised after SE we recorded unitary IPSCs between AC-IN pairs in the hilar-granule cell layer border from rats one week after SE, and in age-matched controls. AC-INs with both HICAP and TML cell morphologies receive synaptic inputs from other AC-INs and FS-BCs, with higher probability of synaptic connections between similar neurons (Savanthrapadian et al., 2014; Yu et al., 2015a). Consistent with earlier observations in HICAP and TML cell pairs (Savanthrapadian et al., 2014; Yu et al., 2015a), synapses between AC-INs showed asynchronous release and short-term facilitation (Fig. 2B and Supplementary Fig. 1). The probability of synaptic connections between physiologically identified AC-IN pairs trended towards an increase after SE, but did not reach statistical significance (Fig. 2B–C, control: 12.0%, 25 pairs in 208 dual recordings; post-SE, 14.9%, 40 pairs in 268 dual recordings, $p=0.36$ by $\chi 2$-test. Note that, given the equal probability of synaptic connections in both directions, each pair of AC-INs was considered as two dual recordings). Unlike AC-IN inputs to FS-BCs (Yu et al., 2015b), reliability of synaptic connections between AC-IN pairs was not different between control and post-SE rats (Fig. 2B, D, Probability of success: con AC-IN→AC-IN: 0.34±0.06, 12 pairs; post-SE AC-IN→AC-IN: 0.37 ±0.04, 25 pairs, $p>0.05$ by Student's *t*-test). Unexpectedly, both the average amplitude of uIPSCs between AC-INs including failures (Fig. 2E, in pA, control: 6.7±1.1, 12 pairs; post-SE: 14.6±3.5, 25 pairs, $p<0.05$ by Student's *t*-test), and uIPSC amplitude potency excluding failures (Fig. 2F, in pA, control: 19.4±2.6, 12 pairs; post-SE: 38.7±5.5, 25 pairs, $p<0.05$ by Student's *t*-test) were significantly increased one week post-SE indicating selective strengthening of synapses between AC-INs. The short-term multi-pulse facilitation of uIPSC amplitude between AC-IN pairs was not different between control and post-SE rats (IPSC3/IPSC1 at 50 Hz, control: 1.47±0.28, 11 pairs; post-SE: 1.12±0.14, 16 pairs, p>0.05 by Student's t-test). Asynchronous release, quantified as the charge transfer measured 15 ms after 8 stimuli at 50 Hz until return to baseline, showed a

trend towards a decrease after SE which did not reach statistical significance (in pA*ms, control: 442.9±224.8 in 10 pairs; post-SE: 111.6±52.5 in 5 pairs, p=0.18 by Student's t-test).

An increase in AC-IN uIPSC amplitude in the absence of changes in release probability or multi-pulse ratio suggests that synapses between AC-INs may show a selective upregulation of post-synaptic receptor numbers. To determine if this is the case, we adopted peak-scaled non-stationary variance analysis (Sigworth, 1980; Traynelis et al., 1993; De Koninck and Mody, 1994; Brickley et al., 1999) to estimate the conductance of receptors underlying AC-IN uIPSCs. Current-variance plots consistently exhibited the characteristic parabolic relationship (Fig. 3A and Supplementary Fig. 2). Single-channel current values were not different between post-SE and control AC-IN uIPSCs (Fig. 3B, in pA, control: 2.2±0.3, 14 pairs; post-SE: 2.1±0.2, 23 pairs, p>0.05 by Mann-Whitney U test) indicating that the $GABA_A$ receptor single-channel conductance is not altered after SE. Additionally, the open probability at peak current was not different between control and post-SE AC-IN pairs (control: 88±8%, 14 pairs; post-SE: 91±7%, 23 pairs, p>0.05 by Mann-Whitney test). However, the number of channels open at peak uIPSC amplitude was consistently enhanced after SE (Fig. 3C, control: 13.6±1.4, 14 pairs; post-SE: 22.5±3.2, 23 pairs, p<0.05 by Mann-Whitney test). These data indicate that the selective strengthening of AC-IN synapses result from a specific increase in the number of $GABA_A$ receptors at synapses between AC-INs.

Cannabinoid modulation of synapses between AC-INs is not altered after SE

CB_1R expressed in the presynaptic terminals of CCK-positive interneurons and TML cells are known to modulate the probability of release at synapses to principal cells and interneurons alike (Freund, 2003; Armstrong and Soltesz, 2012; Yu et al., 2015a). Endogenous cannabinoid signaling can contribute to baseline reduction in synaptic release in the normal brain (Ali, 2007; Neu et al., 2007; Lee et al., 2010). Since cannabinoid regulation of baseline GABA release can be altered following seizures (Chen et al., 2003), we used the specific CB_1R antagonist, AM251 (10 μM) to examine whether basal endocannabinoid modulation of synaptic release between AC-INs is altered after SE. Consistent with the expression of CB_1R in both HICAP and TML cells (Fig 1 A–B and Yu et al., 2015a), the probability of synaptic release in all 12 AC-IN pairs tested (pooled from control and post-SE) was enhanced by AM251 (10 μM, Fig. 4A–C). AM251-induced enhancement of synaptic release between AC-INs was reversible (11 of 11 cells tested) and was not different between control and post-SE rats (Fig. 4D, control: 174.3±14.6% of baseline, 7 pairs; post-SE: 192.4±23% of baseline, 5 pairs, p>0.05 by t-test). As reported previously (Yu et al., 2015), data from pairs in which majority of the axonal arbors of presynaptic AC-INs were recovered and confirmed to be from dendritically projecting TML cells, AM251 consistently enhanced synaptic release by 1.9±0.2 times (range of 1.6–2.2, in n=4 TML→AC-IN pairs compared to 1.3–2.2 in all 7 AC-IN→AC-IN pairs). Similarly, although the average AC-IN uIPSC amplitude (including failures) was higher in post SE rats, AM251 perfusion increased average AC-IN uIPSC amplitude to a similar extent in control and post-SE rats (Fig. 4E, control: 176.7±22.7% of baseline, 6 pairs; post-SE: 201.2±6.0% of baseline, 5 pairs, p=0.25 by t-test). Moreover, individual data points illustrating AM251 enhancement of uIPSC release (Fig. 4D) and amplitude (Fig. 4E) appear tightly clustered around the mean indicating that AC-INs, including dendritically projecting TML cells show similar baseline

CB_1R modulation of release. Crucially, these data demonstrate that baseline endocannabinoid suppression of synaptic release between AC-INs remains unchanged after SE.

Input specificity of SE-induced strengthening of inhibitory synapses to AC-IN

Since AC-INs receive inhibitory connections from FS-BCs (Savanthrapadian et al., 2014), we examined if FS-BC inputs to AC-INs show analogous increases after SE. FS-BCs were distinguished from AC-INs by their characteristic high frequency firing (frequency in Hz at 800 pA current injection, FS-BC: 112.1±7.5, n=12 cells; AC-IN 63.8±6.1, n=25 cells, $p<0.05$ by *t*-test), low input resistance (R_{in}) <150 MΩ (R_{in} in MΩ, FS-BC: 93.0±10.1, n=12 cells; AC-IN 236.9±7.9, n=25 cells, $p<0.05$ by *t*-test) and low spike frequency adaptation (Ratio $ISI_{first/last}$, FS-BC: 0.84±0.04; AC-IN 0.29±0.02, n=25 cells, n=12 cells, $p<0.05$ by *t*-test). FS-BCs expressed parvalbumin and their axons were largely confined to the cell layer (Fig. 5A). As expected, the connection probability between FS-BC→AC-IN pairs was considerably lower than between AC-IN pairs) (Compare Fig. 2C and 5B, also see Savanthrapadian et al., 2014). Similar to synapses between FS-BCs (Bartos et al., 2002; Yu et al., 2015b), FS-BC→AC-IN synapses were characterized by synchronous release (Fig. 5B). One week after pilocarpine-SE, the probability of synaptic connections from physiologically identified FS-BCs to AC-INs showed a small increase that failed to reach statistical significance (Fig. 5C, control: 4.0%, 5 pairs in 125 dual recordings; post-SE: 7.7%, 10 pairs in 130 dual recordings, $p=0.21$ by χ-test). The reliability of synaptic release (Fig. 5D, probability of success: control: 0.57±0. 21%, 3 pairs; post-SE: 0.66±0.13%, 7 pairs, $p>0.05$ by Student's *t*-test) was unaltered after SE. Importantly, the unitary IPSCs (uIPSCs) peak amplitude including failures of at FS-BC→AC-IN synapses was not increased after SE (Fig. 5E, in pA, control: 21.7±20.8, 3 pairs; post-SE: 18.6±7.0, 7 pairs, $p>0.05$ by Student's *t*-test). Similarly, the amplitude potency excluding failures was not increased after SE (in pA, control: 29.0±22.3, 3 pairs, 3 pairs; post-SE: 24.8±5.8, 7 pairs, $p>0.05$ by Student's *t*-test). Note that although, as a consequence of the low connection probability, the amplitude data are from a limited number of FS-BC→AC-IN pairs which showed high variability, amplitude data trended towards a decrease. Thus, unlike synapses between AC-INs, FS-BC inputs to AC-INs are not enhanced after SE. In keeping with the lack of change in release probability at FS-BC→AC-IN synapses (Fig. 5D), short-term depression of uIPSC amplitude observed in FS-BCs synapses on AC-INs was not different between controls and post-SE rats (Fig. 5F, IPSC2/IPSC1 at 50 Hz, control: 0.97±0.34, 3 pairs; post-SE: 0.93±0.09, 7 pairs, p>0.05 by Student's t-test). Therefore, while synapses between AC-INs are strengthened after SE, the characteristic reliability and amplitude of FS-BC inputs to AC-INs remains unchanged.

Unexpected preservation of AC-IN synaptic inhibition after status epilepticus

While we find input specific changes in synaptic inhibition of AC-INs after SE, whether inhibition to AC-INs is altered at the network level is following SE is not known. Previous studies have found a decrease in the frequency of action potential independent mIPSCs in dentate granule cells and FS-BCs after SE (Kobayashi and Buckmaster, 2003; Yu et al., 2015b) which is consistent with the loss of hilar GABAergic neurons (Thind et al., 2010). In contrast to both FS-BCs and granule cells, AC-IN mIPSC inter-event interval (IEI) recorded

in tetrodotoxin (1 μM) was decreased (Fig. 6A–B, IEI in ms, control: median=223.5, IQR=87.8–522.6, n=10 cells; post-SE, median=182.1, IQR=89.7–349.8, n=11 cells, $p<0.05$ K-S test), indicating an increase in AC-IN mIPSC frequency despite loss of hilar interneurons. Consistent with the strengthening of AC-IN synaptic connections, AC-IN mIPSC amplitude increased one week after SE (Fig. 6A–C, in pA, control: median=11.3, IQR=8.2–16.9, n=10 cells; post-SE, median=13.5, IQR=9.1–19.9, n=11 cells, $p<0.05$ K-S test). The early post-SE increase in mIPSC frequency was not sustained and AC-IN mIPSC IEI in epileptic rats was not different from age matched controls (Fig. 6D, mIPSC IEI in ms, control: median=414.9, IQR=153.7–1170.9, n=19 cells; epileptic, median=448.8, IQR=166.9–1052.4, n=17 cells, $p>0.05$ K-S test). However, the enhancement of AC-IN mIPSC amplitude observed after SE persisted in epileptic rats (Fig. 6E, in pA, control: median=10.7, IQR=7.8–16.0, n=19 cells; epileptic, median=14.4, IQR=10.0–20.1, n=17 cells, $p<0.05$ K-S test). Thus, there is an early and persistent increase in AC-IN mIPSC amplitude after SE.

Next we examined whether AC-IN spontaneous synaptic inhibition, which reflects both activity and connectivity from diverse inhibitory neurons, is altered after SE. There was no difference in the IEI of spontaneous inhibitory synaptic currents (sIPSCs) in AC-INs in both post-SE (Fig. 7A–B, sIPSC IEI in ms, control: median=243.1, IQR=105.5.0–501.1, n=16 cells; post-SE, median=232.8, IQR=106.5–583.7, n=15 cells, $p>0.05$ K-S test) and epileptic rats (Figure. 7D, sIPSC IEI in ms, 40 day control: median=206, IQR=89.3–521.1, n=14 cells; epileptic, median=227.3, IQR=86.5–552.7, n=16 cells, $p>0.05$ K-S test). This lack of reduction in AC-IN sIPSC frequency after SE is unexpected as it contrasts with the post-SE decrease in sIPSC frequency in granule cells and FS-BCs (Kobayashi and Buckmaster, 2003; Yu et al., 2015b). AC-IN sIPSC amplitude was significantly enhanced one week after SE (Fig. 7A and C, sIPSC amplitude in pA, control: median=14.7, IQR=9.7–22.9, n=16 cells; post-SE, median=22.2, IQR=14.0–35.7, n=15 cells, $p<0.05$ K-S test) but was not different between epileptic rats and age matched controls (Fig. 7E, sIPSC amplitude in pA, 40 day control: median=18.3, IQR=10.1–31.1, n=14 cells; epileptic, median=18.1, IQR=10.6–23.2, n=16 cells, $p>0.05$ K-S test). The lack of decrease in AC-IN sIPSC frequency and amplitude after SE and in epileptic rats demonstrates that, unlike FS-BCs and granule cells located adjacent to them, synaptic inhibition of AC-INs is not reduced after SE. While the increase in AC-IN sIPSC amplitude 1 week after SE is consistent with strengthening of uIPSCs between AC-INs, the lack of sustained increase in AC-IN sIPSC amplitude in epileptic rats raises the possibility that the changes in AC-IN→AC-IN uIPSC amplitude may be transient. However, since a multitude of changes including altered neuronal activity in non-AC-INs and reorganization of network connectivity could contribute to the overall sIPSC amplitude, the data do not eliminate the possibility of persistent changes in the amplitude of sIPSCs from AC-INs.

Increase in cannabinoid-sensitive inhibition of AC-INs in epilepsy

We decided to use the pharmacological sensitivity of AC-IN synaptic release to CB_1R to directly assess the frequency and amplitude contribution of AC-IN inputs to AC-IN sIPSCs in post-SE and epileptic rats. Since CB_1R modulation of AC-INs was unaltered after SE (Fig. 4), we used the CB_1R agonist, WIN-55212, to selectively suppress release at CB_1R -

positive terminals and examine if the contribution of AC-IN inputs to AC-IN sIPSCs is altered after SE. In control rats, WIN-55212 (WIN) significantly reduced AC-IN sIPSC frequency (in Hz, baseline: 2.9±0.4, WIN: 2.2±0.4, 10 cells, $p<0.05$ by paired Student's *t*-test) indicating that cannabinoid-sensitive inputs contribute to 23.4±3.4% of inhibitory events (Fig. 8A–B, Supplementary Fig. 3A). The proportion of inhibitory events suppressed by WIN increased significantly one week after SE (Fig. 8B, Supplementary Fig. 3A, frequency in Hz, baseline: 3.3±0.9, WIN: 2.4±0.7, 8 cells, $p<0.05$ by paired Student's *t*-test; 37.5±3.2%, $p<0.05$ vs. control by Student's *t*-test). WIN did not decrease sIPSC amplitude in controls (Fig. 8C, Supplementary Fig. 3B, amplitude in pA, baseline: 16.3±2.1, WIN: 16.7±3.1, 10 cells, $p>0.05$ by paired Student's *t*-test). Unlike controls, WIN significantly reduced AC-IN sIPSC amplitude after SE (Fig. 8A and C, Supplementary Fig. 3B, in pA, baseline: 24.5±3.0, WIN: 20.6±2.9, 8 cells, $p<0.05$ by paired Student's *t*-test, 83.6±5.0% of baseline). Since uIPSC amplitude potency at AC-IN→AC-IN synapses tends to be larger than FS-BC→AC-IN after SE (in pA, FS-BC: 24.8±5.8, 7 pairs; AC-IN: 38.7±5.5, 25 pairs, $p>0.05$ by Student's *t*-test), the ability of WIN to decrease the amplitude of sIPSC in AC-INs is consistent with an increase in amplitude of CB_1R-sensitive IPSCs from AC-INs to AC-INs. Finally, we examined whether the increase in CB_1R-sensitive inhibition of AC-INs observed in the post-SE rats persists in epileptic rats. In control rats, examined 45–70 days after saline injection, WIN caused a small decrease in both sIPSC frequency (Fig. 8D and Supplementary Fig. 3C, in Hz, baseline: 4.0±0.9, WIN: 3.4±0.7, in n=9 cells, 88.6±8.0% of baseline, $p>0.05$ by paired Student's *t*-test) and amplitude (Fig. 8E and Supplementary Fig. 3D, in pA, baseline: 24.8±4.4, WIN: 23.5±4.2, in n=9 cells, 94.1±3.8% of baseline, $p>0.05$ by paired Student's *t*-test) in AC-INs which was not significant. WIN significantly reduced sIPSC frequency in AC-INs from epileptic rats >40 days post-SE (Fig. 8D and Supplementary Fig. 3C, in Hz, baseline: 3.5±1.1, WIN: 2.1±0.6, in n=10 cells, 66.7±6.2% of baseline, $p<0.05$ by paired Student's *t*-test) indicating an increase in CB_1R-sensitive IPSCs to dentate AC-INs in epileptic rats. Importantly, WIN significantly reduced AC-IN sIPSC amplitude (Fig. 8E and Supplementary Fig. 3D, in pA, baseline: 21.0±3.2, WIN: 14.7±1.6, in n=10 cells, 76.9±6.7% of baseline, $p<0.05$ by paired Student's *t*-test) in epileptic rats one month after SE demonstrating the persistent increase in amplitude CB_1R-sensitive IPSCs to dentate AC-INs.

Together, these data establish that dentate AC-INs show a unique increase in the proportion and amplitude of mutual CB_1R-sensitive spontaneous synaptic inputs in epilepsy.

Discussion

The major finding of this study concerns cell-type specific changes in the synaptic inhibition of dentate CB_1R-sensitive interneurons after SE. We demonstrate that neuronal populations that contribute to inhibition spanning the molecular layer of the dentate gyrus develop early and persistent enhancement of mutual inhibitory inputs following SE. Our results demonstrate an increase in CB_1R-sensitive inhibition of AC-INs even though both intrinsic excitability of AC-INs and endocannabinoid modulation of synaptic release between AC-INs remained unchanged after SE. Non-stationary variance analysis of uIPSCs between AC-INs one week after SE identified that an increase in the number of $GABA_A$ receptors open at AC-IN uIPSC peak underlies the strengthening of AC-IN synapses. The probability of

finding connected AC-IN pairs was not reduced after SE, suggesting that selective preservation of inhibitory connections between AC-INs could contribute to the unique early post-SE increase in the frequency of mIPSCs and persistent enhancement of CB_1R-sensitive sIPSCs to AC-INs. Since interneuronal synaptic inhibition regulates dynamic network behavior (Chamberland and Topolnik, 2012), the post-SE increase in CB_1R-sensitive synaptic inputs with facilitating short term dynamics and could contribute to paroxysmal alterations in balance between excitation and inhibition and to emergence of seizures.

Laminar organization granule cell inhibition is typified by Chandelier cells inputs to the axon initial segment, FS-BC inputs to the soma, proximal dendritic inhibition by HICAP cells and distal dendritic inhibition by HIPP cells (Soriano et al., 1990; Han et al., 1993; Harney and Jones, 2002; Ewell and Jones, 2010; Hosp et al., 2014). In contrast, TML cells are unique in crossing layers to provide inhibition, albeit sparse, across the molecular layer (Han et al., 1993; Soriano and Frotscher, 1993; Yu et al., 2015a). Although structurally distinct, HICAP and TML cells have similar intrinsic physiology (Yu et al., 2015b; Yu et al., 2015a). Additionally, despite lacking CCK expression, TML cells show CB_1R-modulation of synaptic release (Yu et al., 2015a), a characteristic feature of CCK expressing neurons (Neu et al., 2007). However, unlike dendritically projecting CCK cells in CA1 (Lee et al., 2010), dentate TML cells show baseline CB_1R modulation of synaptic release. Thus dentate CB_1R-sensitive interneurons include two classes of neurons: CCK-expressing/HICAP cells and TML cells, which show similar accommodating intrinsic physiology. Synaptic inputs from AC-INs show asynchronous release (Supplementary Fig. 1) and low release probability which distinguish them from the synchronous and reliable FS-BC and HIPP cells (Bartos et al., 2002; Savanthrapadian et al., 2014; Yu et al., 2015b; Yu et al., 2015a). Moreover, unlike FS-BCs which show depressing short term dynamics, AC-INs show synaptic facilitation which, coupled to their asynchronous release, is suited to maintain a sustained inhibitory tone during network activity (Hefft and Jonas, 2005; Yu et al., 2015b; Yu et al., 2015a). While CB_1R-sensitive inhibition of FS-BCs is reduced after SE (Yu et al., 2015b), we demonstrate that CB_1R-sensitive inhibitory inputs to AC-INs show early and persistent enhancement after SE. This also contrasts with decrease in CB_1R-sensitive granule cell inhibition observed in epilepsy (Sun et al., 2014) and suggests that selective sparing or sprouting of AC-IN synaptic interconnection may occur after SE. Thus CB_1R-sensitive AC-INs appear to have a have distinct role in the dentate circuit both under normal conditions and in epilepsy.

Previous studies have shown that granule cell and FS-BC mIPSC frequency is decreased after SE (Kobayashi and Buckmaster, 2003; Yu et al., 2015b), which is consistent with early loss of hilar interneurons, particularly the somatostatin expressing HIPP cells (Thind et al., 2010). Despite ongoing cell loss and decrease in CCK- axon terminals after SE (Thind et al., 2010; Sun et al., 2014), we find that AC-IN mIPSC frequency is increased in rats 1 week post-SE. These data contrast with the decrease in mIPSC frequency observed in FS-BCs under identical experimental conditions (Yu et al., 2013; Yu et al., 2015b). A potential reason for the lack of post-SE decrease in AC-IN mIPSCs is that, unlike granule cells and FS-BCs, AC-INs receive limited synaptic inputs from the population of HIPP cells vulnerable to loss following SE (Kobayashi and Buckmaster, 2003; Savanthrapadian et al., 2014). Additionally, while not statistically significant, the small increase in the probability

of FS-BC and AC-IN connections to AC-INs in our paired recordings together with the early evidence for increase in mIPSC frequency (Fig. 6) suggest an increase in inhibitory synaptic connections to AC-INs after SE. Curiously, despite the early increase in AC-IN mIPSC frequency after SE and although AC-IN intrinsic excitability, synaptic release probability and baseline cannabinoid tone are not reduced, AC-IN sIPSC frequency was not increased early after SE. Since CB_1R-sensitive events contribute to a greater proportion of sIPSCs after SE (Fig. 8), the lack of increase in sIPSC frequency despite increase in mIPSC frequency suggests that action-potential driven IPSC from FS-BCs and other interneurons innervating AC-INs may be reduced after SE. Because both FS-BC intrinsic excitability (Yu et al., 2015b) and reliability of FS-BC synapses to AC-INs (Fig. 5) are not altered after SE, it is possible that previously identified decreases in excitatory drive to FS-BCs (Zhang and Buckmaster, 2009) may reduce network-driven FS-BC firing and spontaneous inhibitory inputs to AC-INs.

Unlike post-SE rats, AC-IN mIPSC frequency was not different between controls and epileptic rats. This parallels the lack of difference in FS-BC mIPSC frequency in epileptic rats (Yu et al., 2015b) and may be a consequence of progressive structural plasticity of inhibitory networks (Zhang et al., 2009; Peng et al., 2013). Of note, while the early increase in AC-IN mIPSC frequency is no longer evident >40 days after SE, FS-BC show an early decrease after SE which recovers to control levels at later time points demonstrating that inhibitory inputs to AC-INs and FS-BCs show diametrically opposite changes with time after SE. Additionally, similar to the findings in post-SE rats, AC-IN sIPSC frequency in epileptic rats was not different from controls. Once again, these findings differ from the early and persistent decrease in FS-BC sIPSC frequency after SE (Yu et al., 2013; Yu et al., 2015b). Overall, our examination of AC-IN mIPSC and sIPSC frequency has identified that the SE-induced early and long-term changes in AC-IN synaptic inhibition are distinct from those observed in FS-BCs, revealing a novel cell-type specific reorganization of inhibitory inputs to dentate interneurons following SE. Importantly, we demonstrate a persistent increase in AC-IN mIPSC amplitude after SE and in epileptic rats. However, the early increase in AC-IN sIPSC amplitude was not sustained in epileptic rats. Our paired AC-IN recordings conducted one week after SE show that the amplitude of AC-IN→AC-IN synapses nearly doubled after SE indicating that the larger mIPSC amplitude observed after SE could arise from AC-INs inputs. Similarly, the ability of WIN to consistently suppress AC-IN sIPSC amplitude one week and >40 days after SE but not in controls confirms that, following SE, CB_1R-sensitive sIPSCs to AC-INs are larger than average. Thus although AC-IN to AC-IN uIPSC amplitude was not directly examined in epileptic rats, our data demonstrating an increase in CB_1R-sensitive sIPSCs to AC-INs in epileptic rats is consistent with a persistent increase in amplitude of synapse between AC-INs after SE. It is possible that simultaneous SE-induced or compensatory alterations in activity of CB_1R-insensitive neurons or their synaptic strengths could have contributed to reducing AC-IN sIPSC amplitude to control levels in epileptic rats.

Non-stationary variance analysis on uIPSCs in paired AC-IN recordings showed that neither single channel current nor peak open probability were altered one week after SE. In contrast, the number of channels open at the peak was increased after SE. Curiously, the measures average peak uIPSC amplitude in both control and post-SE pairs was lower than the

amplitude calculated based on average single channel current and the number of channels estimated from fits. Although the source of this variability is unclear, our selection of successful uIPSCs for analysis and the absence of trial-to-trial variability in uIPSC amplitude suggestive of multiple synapses between the recorded neurons, rule out potential presynaptic mechanisms such as branch-point failure. Additionally since the peak open probability was not altered after SE, we suggest that a specific increase in post-synaptic $GABA_A$ receptor numbers at AC-IN synapses, rather than changes in receptor affinity or vesicle content, underlies the increase in unitary IPSCs amplitude at synapses between AC-INs measured one week after SE.

Endocannabinoid signaling regulates both excitatory and inhibitory synaptic release in the dentate molecular layer. Glutamatergic mossy cell synapses in the IML show cannabinoid-mediated suppression of glutamate release (Monory et al., 2006) which has been suggested to reduce the severity of acute kainic acid induced seizures (Marsicano et al., 2003; Monory et al., 2006). Thus the endocannabinoid system has been suggested as a valuable target for seizure termination and epilepsy treatment (Hofmann and Frazier, 2013). However, because the endocannabinoid system undergoes plasticity in epilepsy (Magloczky et al., 2010; Karlocai et al., 2011), anti-epileptic drugs targeting the cannabinoid and inhibitory systems need to function in the modified network. While there is evidence for increases in CB_1Rs at dentate GABAergic terminals in epilepsy (Magloczky et al., 2010), the density of CCK-positive terminals and cannabinoid-sensitive inhibition of granule cells is reduced in epilepsy (Sun et al., 2014). Our results showing an increase in cannabinoid-sensitive inhibition of AC-INs suggest that the post-SE enhancement of CB_1R (Magloczky et al., 2010) may reflect increases in AC-IN connectivity in epilepsy. This unique strengthening of CB_1R-sensitive inhibition between AC-INs could reduce AC-IN firing. Therefore, in addition to the structural loss of CCK inputs to granule cells (Sun et al., 2014), enhanced mutual inhibition between AC-INs could lead to a functional decrease in the cannabinoid-sensitive inhibition of granule cells. Since cannabinoid modulation of inhibition impacts network rhythms (Hajos et al., 2000; Reich et al., 2005), enhanced mutual inhibition between AC-INs in epilepsy is likely to alter network oscillatory patterns.

Apart from steady-state effects, frequency-dependent relief from cannabinoid suppression of release (Foldy et al., 2006; Neu et al., 2007) together with the facilitating short-term dynamics of the AC-IN synapses could contribute to episodic ebb and flow in activity of interconnected AC-INs. Additionally, activity-dependent changes in the recruitment of AC-INs can dynamically modify the functional heterogeneity of inhibition and impact network activity and oscillations (Aradi et al., 2004). Arguably, the decrease in CB_1R-sensitive inhibition of granule cells in epilepsy (Sun et al., 2014) may dampen the effects of dynamic changes in inhibition and disinhibition of AC-INs on network excitability. However, since FS-BC inputs tend to depress during sustained activation (Hefft and Jonas, 2005), as would occur during seizures, facilitating asynchronous inhibition from AC-INs is likely to significantly limit principal cell activity during seizures. In this regard, genetic deletion of CB_1R in inhibitory neurons reduces the duration of after-discharges following kindling (von Ruden et al., 2014), indicating a role for CB_1R-sensitive inhibition in seizure termination. The identification of increased CB_1R availability in spatial and temporal proximity to seizure initiation zone in epileptic patients (Goffin et al., 2011) together with our

demonstration of enhanced CB_1R-sensitive AC-IN inhibition, is consistent with the proposal that upregulation of interneuronal CB_1R may predispose to development of an epileptogenic zone (Goffin et al., 2011). Since AC-INs are positioned to undergo feed-forward activation by entorhinal and associational inputs, enhanced asynchronous and facilitating mutual inhibition between AC-INs would be expected to limit AC-IN firing during dentate activation. The ensuing intermittent collapse in asynchronous and sustained feed-forward and feed-back inhibition of granule cells, will likely render the dentate permissive to seizure initiation and propagation. Furthermore, the changes in CB_1R-sensitive inhibition reported here will impact the network function of anti-epileptics targeting the endocannabinoid system.

In summary, using rigorous single cell and paired interneuronal recordings, our study demonstrates a novel increase in cannabinoid-sensitive inhibition of dentate accommodating interneurons after experimental SE, which could cause activity-dependent alterations in dentate inhibition during epileptogenesis and in epilepsy.

Supplementary Material

Refer to Web version on PubMed Central for supplementary material.

Acknowledgments

This work is supported by Epilepsy Foundation Grants to J.Y. and NIH/NINDS R01 NS069861 and CURE Foundation to V.S.

Abbreviations

AC-IN	Accommodating Interneuron
ACSF	Artificial cerebrospinal fluid
CB_1R	Cannabinoid receptor type 1
CCK	cholecystokinin
FS-BC	fast-spiking basket cell
HIPP cell	hilar-perforant pathway-associated cell
HICAP cell	Hilar commissural-associational pathway-associated cell
IEI	inter-event interval
IQR	interquartile range
IML	Inner molecular layer
mIPSC	miniature inhibitory postsynaptic current
PV	Parvalbumin
sIPSC	spontaneous inhibitory postsynaptic current
TML cell	Total molecular layer cell

uIPSC unitary inhibitory postsynaptic current

Reference List

Ali AB. Presynaptic Inhibition of GABAA receptor-mediated unitary IPSPs by cannabinoid receptors at synapses between CCK-positive interneurons in rat hippocampus. J Neurophysiol. 2007; 98:861–869. [PubMed: 17567776]

Aradi I, Santhakumar V, Soltesz I. Impact of heterogeneous perisomatic IPSC populations on pyramidal cell firing rates. J Neurophysiol. 2004; 91:2849–2858. [PubMed: 15136604]

Armstrong C, Soltesz I. Basket cell dichotomy in microcircuit function. J Physiol. 2012; 590:683–694. [PubMed: 22199164]

Bartos M, Vida I, Frotscher M, Meyer A, Monyer H, Geiger JR, Jonas P. Fast synaptic inhibition promotes synchronized gamma oscillations in hippocampal interneuron networks. Proceedings of the National Academy of Sciences of the United States of America. 2002; 99:13222–13227. [PubMed: 12235359]

Brickley SG, Cull-Candy SG, Farrant M. Single-channel properties of synaptic and extrasynaptic GABAA receptors suggest differential targeting of receptor subtypes. J Neurosci. 1999; 19:2960–2973. [PubMed: 10191314]

Buckmaster PS, Jongen-Relo AL. Highly specific neuron loss preserves lateral inhibitory circuits in the dentate gyrus of kainate-induced epileptic rats. J Neurosci. 1999; 19:9519–9529. [PubMed: 10531454]

Chamberland S, Topolnik L. Inhibitory control of hippocampal inhibitory neurons. Front Neurosci. 2012; 6:165. [PubMed: 23162426]

Chen K, Ratzliff A, Hilgenberg L, Gulyas A, Freund TF, Smith M, Dinh TP, Piomelli D, Mackie K, Soltesz I. Long-term plasticity of endocannabinoid signaling induced by developmental febrile seizures. Neuron. 2003; 39:599–611. [PubMed: 12925275]

Coulter DA. Chronic epileptogenic cellular alterations in the limbic system after status epilepticus. Epilepsia. 1999; 40(Suppl 1):23–33.

Craft RM, Marusich JA, Wiley JL. Sex differences in cannabinoid pharmacology: a reflection of differences in the endocannabinoid system? Life Sci. 2013; 92:476–481. [PubMed: 22728714]

De Koninck Y, Mody I. Noise analysis of miniature IPSCs in adult rat brain slices: properties and modulation of synaptic GABAA receptor channels. J Neurophysiol. 1994; 71:1318–1335. [PubMed: 8035217]

Devinsky O, Cilio MR, Cross H, Fernandez-Ruiz J, French J, Hill C, Katz R, Di Marzo V, Jutras-Aswad D, Notcutt WG, Martinez-Orgado J, Robson PJ, Rohrback BG, Thiele E, Whalley B, Friedman D. Cannabidiol: pharmacology and potential therapeutic role in epilepsy and other neuropsychiatric disorders. Epilepsia. 2014; 55:791–802. [PubMed: 24854329]

Echegoyen J, Armstrong C, Morgan RJ, Soltesz I. Single application of a CB1 receptor antagonist rapidly following head injury prevents long-term hyperexcitability in a rat model. Epilepsy Res. 2009; 85:123–127. [PubMed: 19369036]

Ewell LA, Jones MV. Frequency-tuned distribution of inhibition in the dentate gyrus. The Journal of neuroscience: the official journal of the Society for Neuroscience. 2010; 30:12597–12607. [PubMed: 20861366]

Foldy C, Neu A, Jones MV, Soltesz I. Presynaptic, activity-dependent modulation of cannabinoid type 1 receptor-mediated inhibition of GABA release. J Neurosci. 2006; 26:1465–1469. [PubMed: 16452670]

Freund TF. Interneuron Diversity series: Rhythm and mood in perisomatic inhibition. Trends Neurosci. 2003; 26:489–495. [PubMed: 12948660]

Goffin K, Van Paesschen W, Van Laere K. In vivo activation of endocannabinoid system in temporal lobe epilepsy with hippocampal sclerosis. Brain. 2011; 134:1033–1040. [PubMed: 21303859]

Gupta A, Elgammal FS, Proddutur A, Shah S, Santhakumar V. Decrease in Tonic Inhibition Contributes to Increase in Dentate Semilunar Granule Cell. Journal of Neuroscience. 2012; 32:2523–2537. [PubMed: 22396425]

Hajos N, Katona I, Naiem SS, MacKie K, Ledent C, Mody I, Freund TF. Cannabinoids inhibit hippocampal GABAergic transmission and network oscillations. Eur J Neurosci. 2000; 12:3239–3249. [PubMed: 10998107]

Han ZS, Buhl EH, Lorinczi Z, Somogyi P. A High-Degree of Spatial Selectivity in the Axonal and Dendritic Domains of Physiologically Identified Local-Circuit Neurons in the Dentate Gyrus of the Rat Hippocampus. European Journal of Neuroscience. 1993; 5:395–410. [PubMed: 8261117]

Harney SC, Jones MV. Pre- and postsynaptic properties of somatic and dendritic inhibition in dentate gyrus. Neuropharmacology. 2002; 43:584–594. [PubMed: 12367604]

Hefft S, Jonas P. Asynchronous GABA release generates long-lasting inhibition at a hippocampal interneuron-principal neuron synapse. Nat Neurosci. 2005; 8:1319–1328. [PubMed: 16158066]

Hofmann ME, Frazier CJ. Marijuana, endocannabinoids, and epilepsy: potential and challenges for improved therapeutic intervention. Exp Neurol. 2013; 244:43–50. [PubMed: 22178327]

Hosp JA, Struber M, Yanagawa Y, Obata K, Vida I, Jonas P, Bartos M. Morpho-physiological criteria divide dentate gyrus interneurons into classes. Hippocampus. 2014; 24:189–203. [PubMed: 24108530]

Karlocai MR, Toth K, Watanabe M, Ledent C, Juhasz G, Freund TF, Magloczky Z. Redistribution of CB1 cannabinoid receptors in the acute and chronic phases of pilocarpine-induced epilepsy. PLoS One. 2011; 6:e27196. [PubMed: 22076136]

Kobayashi M, Buckmaster PS. Reduced inhibition of dentate granule cells in a model of temporal lobe epilepsy. J Neurosci. 2003; 23:2440–2452. [PubMed: 12657704]

Lee SH, Foldy C, Soltesz I. Distinct endocannabinoid control of GABA release at perisomatic and dendritic synapses in the hippocampus. J Neurosci. 2010; 30:7993–8000. [PubMed: 20534847]

Li Y, Korgaonkar AA, Swietek B, Wang J, Elgammal FS, Elkabes S, Santhakumar V. Toll-like receptor 4 enhancement of non-NMDA synaptic currents increases dentate excitability after brain injury. Neurobiol Dis. 2014; 74C:240–253. [PubMed: 25497689]

Magloczky Z, Toth K, Karlocai R, Nagy S, Eross L, Czirjak S, Vajda J, Rasonyi G, Kelemen A, Juhos V, Halasz P, Mackie K, Freund TF. Dynamic changes of CB1-receptor expression in hippocampi of epileptic mice and humans. Epilepsia. 2010; 51(Suppl 3):115–120. [PubMed: 20618415]

Maguire J, Mody I. Neurosteroid synthesis-mediated regulation of GABA(A) receptors: relevance to the ovarian cycle and stress. J Neurosci. 2007; 27:2155–2162. [PubMed: 17329412]

Marsicano G, Goodenough S, Monory K, Hermann H, Eder M, Cannich A, Azad SC, Cascio MG, Gutierrez SO, van der Stelt M, Lopez-Rodriguez ML, Casanova E, Schutz G, Zieglgansberger W, Di Marzo V, Behl C, Lutz B. CB1 cannabinoid receptors and on-demand defense against excitotoxicity. Science. 2003; 302:84–88. [PubMed: 14526074]

Monory K, et al. The endocannabinoid system controls key epileptogenic circuits in the hippocampus. Neuron. 2006; 51:455–466. [PubMed: 16908411]

Morozov YM, Torii M, Rakic P. Origin, early commitment, migratory routes, and destination of cannabinoid type 1 receptor-containing interneurons. Cereb Cortex. 2009; 19(Suppl 1):i78–89. [PubMed: 19346272]

Mott DD, Turner DA, Okazaki MM, Lewis DV. Interneurons of the dentate-hilus border of the rat dentate gyrus: morphological and electrophysiological heterogeneity. J Neurosci. 1997; 17:3990–4005. [PubMed: 9151716]

Neu A, Foldy C, Soltesz I. Postsynaptic origin of CB1-dependent tonic inhibition of GABA release at cholecystokinin-positive basket cell to pyramidal cell synapses in the CA1 region of the rat hippocampus. J Physiol. 2007; 578:233–247. [PubMed: 17053036]

Ohno-Shosaku T, Maejima T, Kano M. Endogenous cannabinoids mediate retrograde signals from depolarized postsynaptic neurons to presynaptic terminals. Neuron. 2001; 29:729–738. [PubMed: 11301031]

Peng Z, Zhang N, Wei W, Huang CS, Cetina Y, Otis TS, Houser CR. A reorganized GABAergic circuit in a model of epilepsy: evidence from optogenetic labeling and stimulation of somatostatin interneurons. J Neurosci. 2013; 33:14392–14405. [PubMed: 24005292]

Proddutur A, Yu J, Elgammal FS, Santhakumar V. Seizure-induced alterations in fast-spiking basket cell GABA currents modulate frequency and coherence of gamma oscillation in network simulations. Chaos. 2013; 23:046109. [PubMed: 24387588]

Reich CG, Karson MA, Karnup SV, Jones LM, Alger BE. Regulation of IPSP theta rhythm by muscarinic receptors and endocannabinoids in hippocampus. J Neurophysiol. 2005; 94:4290–4299. [PubMed: 16093334]

Savanthrapadian S, Meyer T, Elgueta C, Booker SA, Vida I, Bartos M. Synaptic Properties of SOM- and CCK-Expressing Cells in Dentate Gyrus Interneuron Networks. J Neurosci. 2014; 34:8197–8209. [PubMed: 24920624]

Sigworth FJ. The variance of sodium current fluctuations at the node of Ranvier. J Physiol. 1980; 307:97–129. [PubMed: 6259340]

Soriano E, Frotscher M. GABAergic innervation of the rat fascia dentata: a novel type of interneuron in the granule cell layer with extensive axonal arborization in the molecular layer. J Comp Neurol. 1993; 334:385–396. [PubMed: 8376624]

Soriano E, Nitsch R, Frotscher M. Axo-axonic chandelier cells in the rat fascia dentata: Golgi-electron microscopy and immunocytochemical studies. J Comp Neurol. 1990; 293:1–25. [PubMed: 1690225]

Sun C, Sun J, Erisir A, Kapur J. Loss of cholecystokinin-containing terminals in temporal lobe epilepsy. Neurobiol Dis. 2014; 62:44–55. [PubMed: 24051276]

Thind KK, Yamawaki R, Phanwar I, Zhang G, Wen X, Buckmaster PS. Initial loss but later excess of GABAergic synapses with dentate granule cells in a rat model of temporal lobe epilepsy. J Comp Neurol. 2010; 518:647–667. [PubMed: 20034063]

Traynelis SF, Silver RA, Cull-Candy SG. Estimated conductance of glutamate receptor channels activated during EPSCs at the cerebellar mossy fiber-granule cell synapse. Neuron. 1993; 11:279–289. [PubMed: 7688973]

von Ruden EL, Jafari M, Bogdanovic RM, Wotjak CT, Potschka H. Analysis in conditional cannabinoid 1 receptor-knockout mice reveals neuronal subpopulation-specific effects on epileptogenesis in the kindling paradigm. Neurobiol Dis. 2014; 73:334–347. [PubMed: 25123336]

Wallace MJ, Blair RE, Falenski KW, Martin BR, DeLorenzo RJ. The endogenous cannabinoid system regulates seizure frequency and duration in a model of temporal lobe epilepsy. J Pharmacol Exp Ther. 2003; 307:129–137. [PubMed: 12954810]

Wyeth MS, Zhang N, Mody I, Houser CR. Selective reduction of cholecystokinin-positive basket cell innervation in a model of temporal lobe epilepsy. J Neurosci. 2010; 30:8993–9006. [PubMed: 20592220]

Yu J, Swietek B, Proddutur A, Santhakumar V. Dentate total molecular layer interneurons mediate cannabinoid-sensitive inhibition. Hippocampus. 2015a; 25:884–889. [PubMed: 25603947]

Yu J, Proddutur A, Elgammal FS, Ito T, Santhakumar V. Status epilepticus enhances tonic GABA currents and depolarizes GABA reversal potential in dentate fast-spiking basket cells. J Neurophysiol. 2013; 109:1746–1763. [PubMed: 23324316]

Yu J, Proddutur A, Swietek B, Elgammal FS, santhakumar V. Functional reduction in Cannabinoid-Sensitive Heterotypic Inhibition of Dentate Basket Cells in Epilepsy: Impact on Network Rhythms. Cereb Cortex. 2015b10.1093/cercor/bhv199

Zhang N, Wei W, Mody I, Houser CR. Altered localization of GABA(A) receptor subunits on dentate granule cell dendrites influences tonic and phasic inhibition in a mouse model of epilepsy. J Neurosci. 2007; 27:7520–7531. [PubMed: 17626213]

Zhang W, Buckmaster PS. Dysfunction of the dentate basket cell circuit in a rat model of temporal lobe epilepsy. J Neurosci. 2009; 29:7846–7856. [PubMed: 19535596]

Zhang W, Yamawaki R, Wen X, Uhl J, Diaz J, Prince DA, Buckmaster PS. Surviving hilar somatostatin interneurons enlarge, sprout axons, and form new synapses with granule cells in a mouse model of temporal lobe epilepsy. J Neurosci. 2009; 29:14247–14256. [PubMed: 19906972]

Highlights

- Basic physiology of dentate accommodating interneurons is unaltered in epilepsy
- Status epilepticus strengthens synapses between accommodating interneurons
- Status epilepticus increases GABA receptors at synapses between AC-INs
- Synaptic inhibition to accommodating interneurons is not reduced in epilepsy
- Cannabinoid-sensitive inhibition of AC-INs is increased in epilepsy

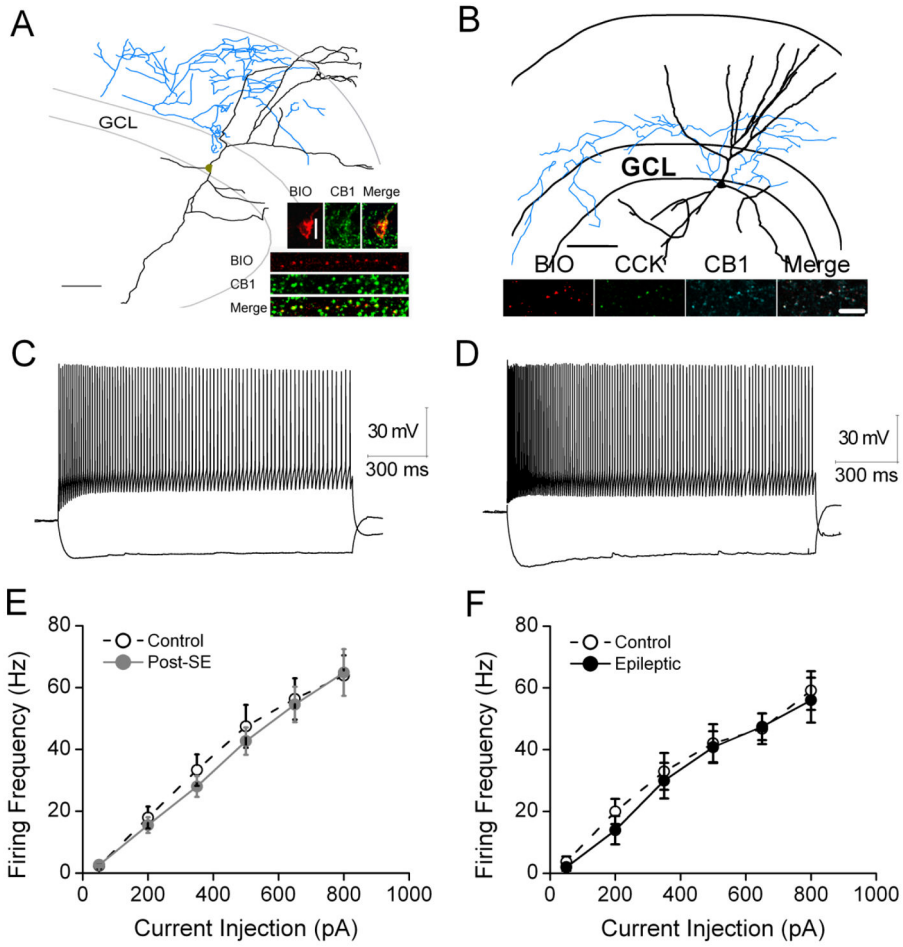

Figure 1. Firing characteristics of AC-INs are not modified after SE

(A): Neurolucida reconstruction of an AC-IN with TML-like morphology shows axon collaterals (blue) spanning the molecular layer. Scale bar, 100 μm. Insets: Confocal images of biocytin-filled soma (red, top left panel), labeling for CB_1R (green, top middle) and merged image (top right). Lower inset shows biocytin-filled axon in the molecular layer (red, upper), labeling for CB_1R (green, top middle) and merge (lower). Scale bar, 20 μm. (B): Reconstruction of a HICAP-like AC-IN with axon (blue) in inner molecular layer. Scale bar, 100 μm. Insets: Confocal image of biocytin-filled axon (red) and labeling for CCK (green), CB_1R (blue) and merged image (left) shows co-labeling in axon. Scale bar, 20 μm. (C–D): Representative membrane voltage traces show firing pattern in a TML (C) and HICAP cell (D) during +500pA and −100 pA current injections. (E): Overlay of current-firing (I/F) curves from AC-INs in control and post-SE rats. (F): Comparison of the current-firing (I/F) curves from AC-INs in epileptic rats and age-matched controls.

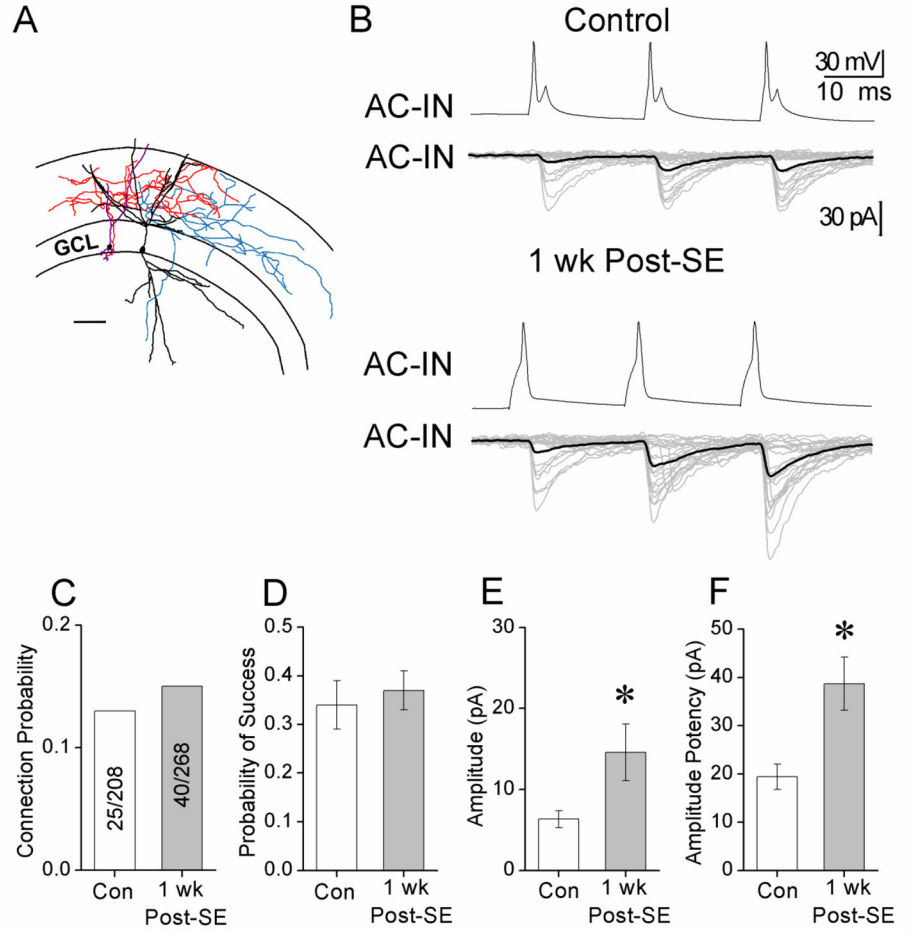

Figure 2. Strengthening of unitary IPSCs between AC-INs 1 week post-SE

(A): Neurolucida reconstruction of a pair of AC-INs with TML-like morphology. Note the sparse axon collaterals extending throughout the molecular layer. Scale bar, 100 μm. GC: granule cell layer. Axons and dendrites of the neurons are illustrated in different colors. (B): Action potentials in presynaptic AC-IN (upper traces) evoke IPSC (lower traces, 30 sweeps in gray and average in black) in the synaptically connected AC-IN in control (upper panel) and post-SE (lower panel) rats. Note the increase in amplitude of IPSC2 and IPSC3 compared to IPSC1 (C–F): Summary plots of the probability of synaptic connections among recorded AC-IN to AC-IN pairs (C), success rate of synaptic release (D), average uIPSC amplitude including failures and (E), peak amplitude of successful uIPSCs (F).

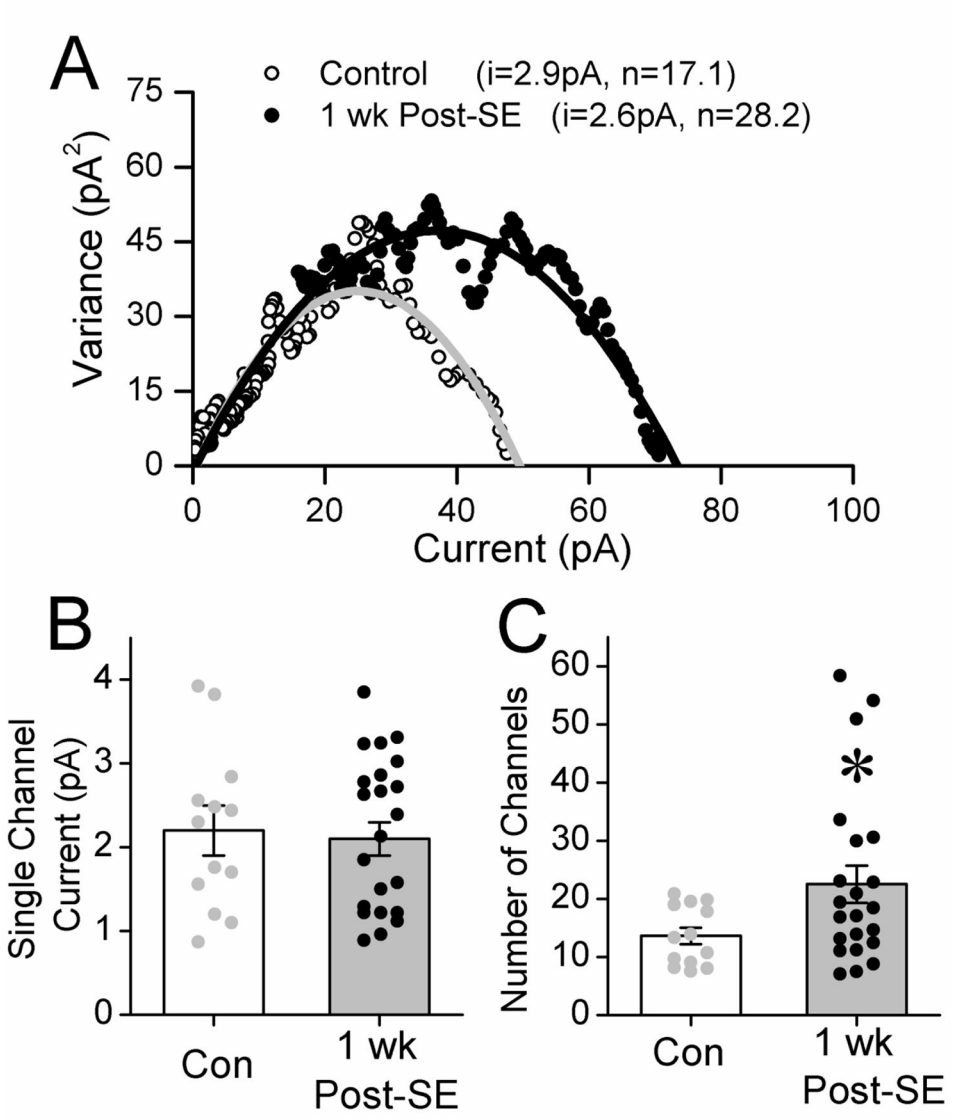

Figure 3. Increase in postsynaptic $GABA_A$ receptors at AC-IN synapses

(A): Plots of mean current against variance from uIPSCs obtained during paired recordings from AC-INs in control (○) and post-SE (●) rats. The plots are fit with parabolic curves to give the weighted-mean single-channel current (i) and number of channels open at the peak (N_P). (B–C): Histograms of weighted-mean single-channel currents (B) and number of channels open at the peak (C) in AC-IN pairs from control and post-SE rats. (*$p<0.05$, t-test).

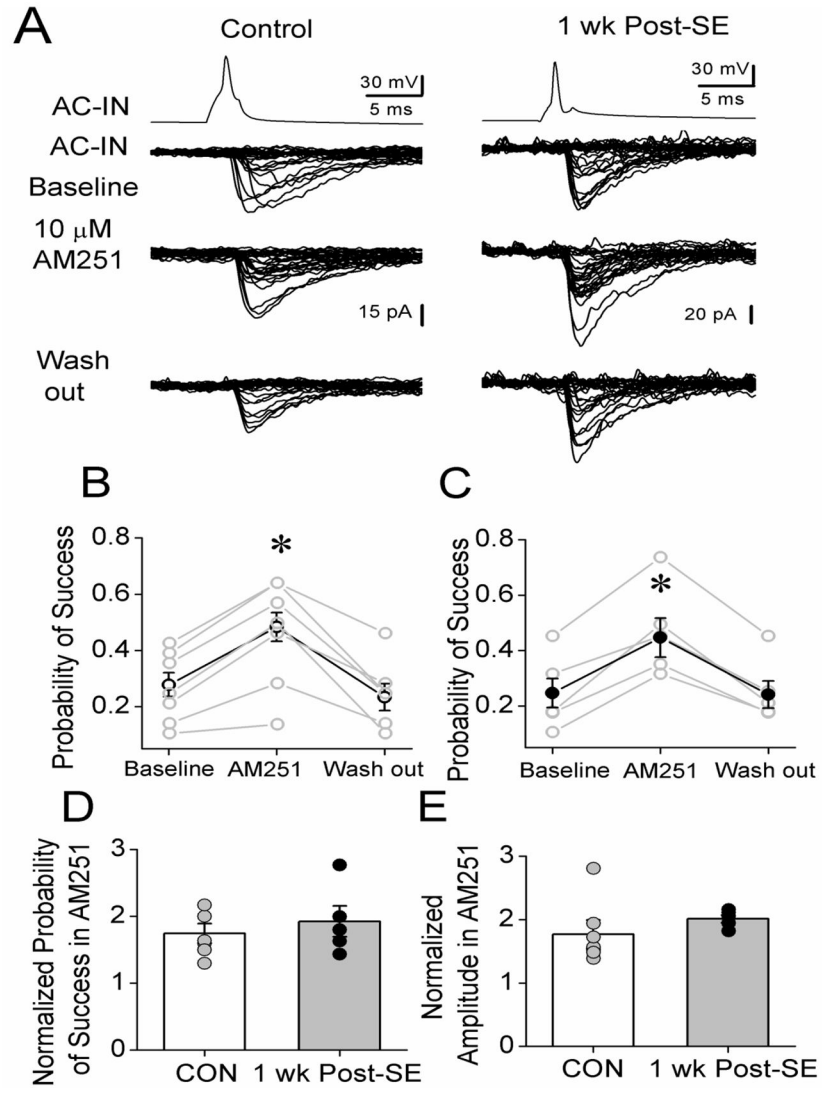

Figure 4. CB_1R modulation of synaptic release between AC-INs is unchanged in post-SE rats

(A): Consecutive uIPSCs traces evoked by presynaptic firing at synapses between AC-INs in control aCSF (baseline), during perfusion of the CB_1R antagonist AM251 (10 μM) and during drug washout in control (left panel) and post-SE (right panel) rats. Note that AM251 reduced the number of failures in both pairs. (B–C): Summary data show the effect of AM251 on the success rate of AC-IN→AC-IN synapses in both control (○, B) and post-SE (●, C) rats. Note the recovery after drug wash out (individual pairs are in gray and average is in black, *$p<0.05$, paired t-test, compared to baseline). (D–E): Summary plots compare the effect of AM251 on success rate (D, normalized to baseline) and amplitude (E, normalized to baseline) in AC-IN pairs from control and post-SE rats.

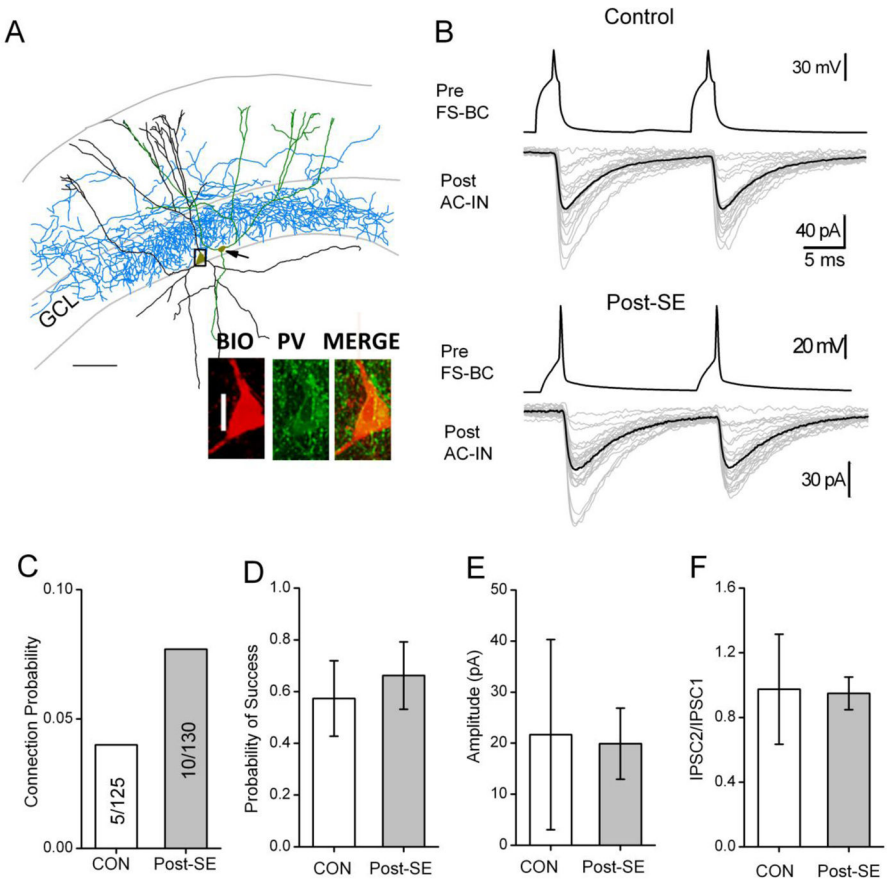

Figure 5. Unitary IPSCs from FS-BC to AC-IN are not altered after SE

(A): Reconstruction of a presynaptic FS-BC with axon (blue) in granule cell layer (GC) and postsynaptic AC-IN (arrow) with axon in the IML. Insets: Confocal image of biocytin-filled FS-BC soma (red) and labeling for parvalbumin (PV, green). Merged image (left) shows PV and biocytin co-labeling in the soma. (B): Example voltage traces above from presynaptic FS-BCs show action potentials (50 Hz). Current traces below show unitary IPSCs (30 sweeps in gray and averaged traces in black) in the synaptically connected AC-IN from control (left panel) and post-SE (right panel) rats. (C–F): Summary plots of the probability of synaptic connections among recorded FS-BC to AC-IN pairs (C), success rate of synaptic release (D), average uIPSC amplitude including failures (E) and paired-pulse ratio in response to 50Hz firing in presynaptic FS-BC (F).

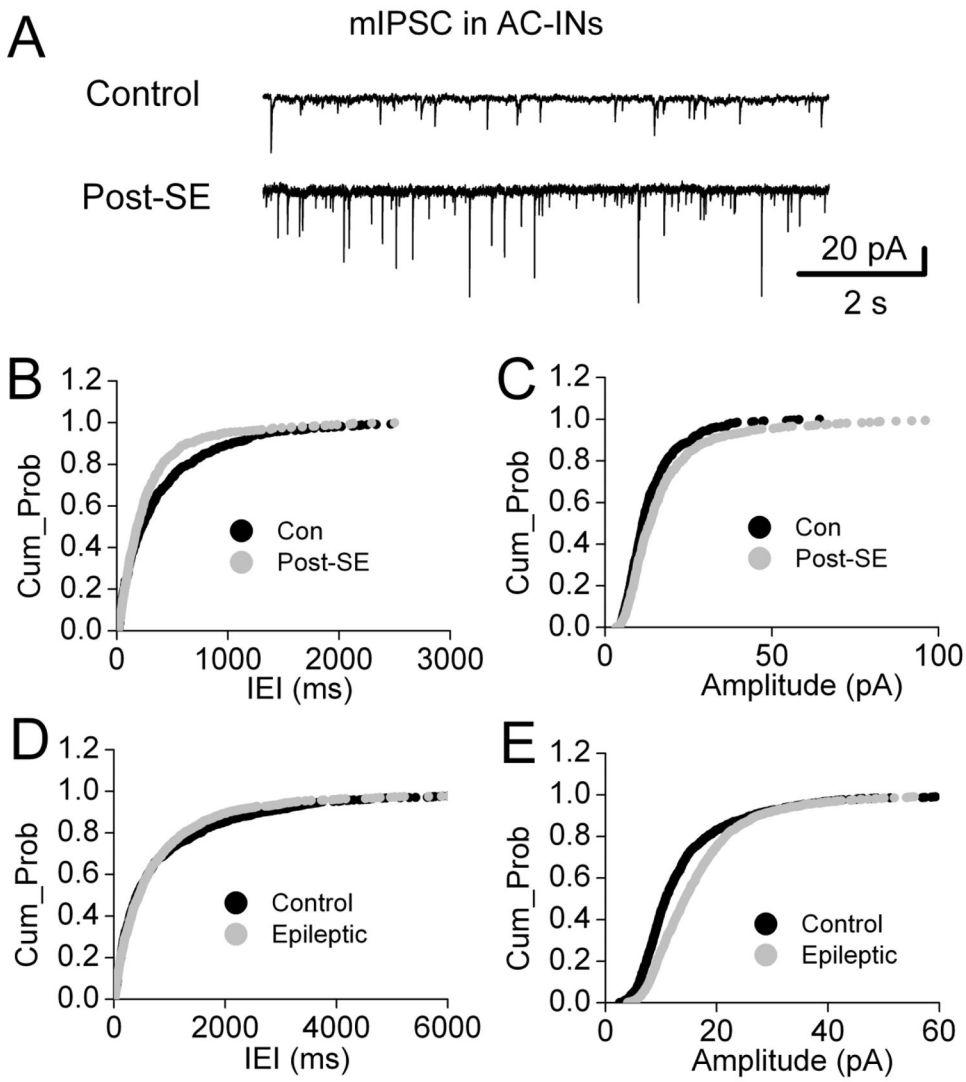

Figure 6. AC-INs show increase in mIPSC amplitude after SE

(A): Representative current traces show mIPSC recorded in the presence of 1μM tetrodotoxin in AC-INs from control (upper trace) and post-SE (lower trace). (B–C): Cumulative probability plot of AC-IN mIPSC inter-event intervals (B) shows a decrease ($P<0.05$, K-S test), and amplitude (C) an increase ($P<0.05$, K-S test), one week after SE (Post-SE) compared to age-matched control rats (Con). (D–E): Cumulative probability distributions of inter-event intervals (D, $P>0.05$, K-S test) and amplitude (E, $P<0.05$, K-S test) of mIPSCs from epileptic and age-matched control rats.

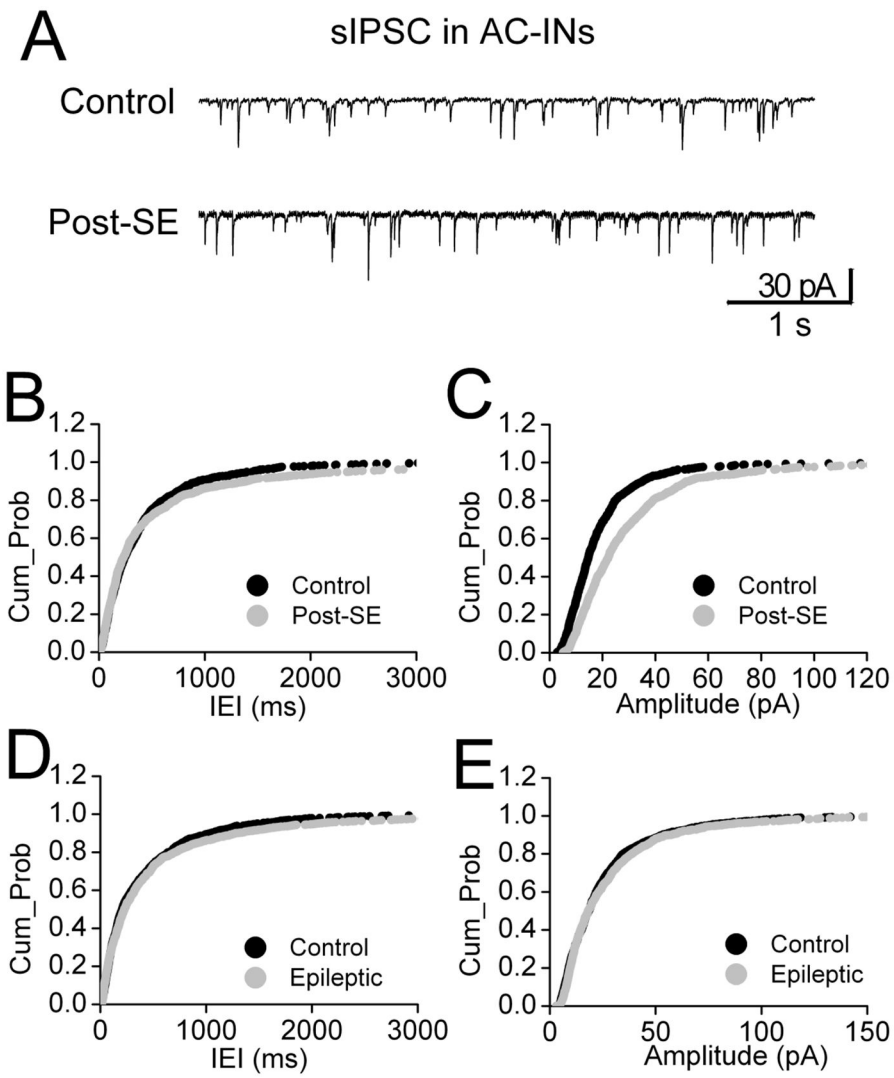

Figure 7. Dentate AC-IN sIPSCs IEI is not altered in post-SE and epileptic rats

(A): Voltage clamp recordings of AC-INs from control (upper trace) and post-SE (lower trace) rats. (B–C): Cumulative probability plots of frequency (B, P>0.05, K-S test) and amplitude (C, P<0.05, K-S test) of sIPSCs in AC-INs from post-SE and control rats. (D–E): Cumulative probability plot of frequency (D, P>0.05, K-S test) and amplitude (E, P>0.05, K-S test) of sIPSCs from epileptic and age-matched control rats.

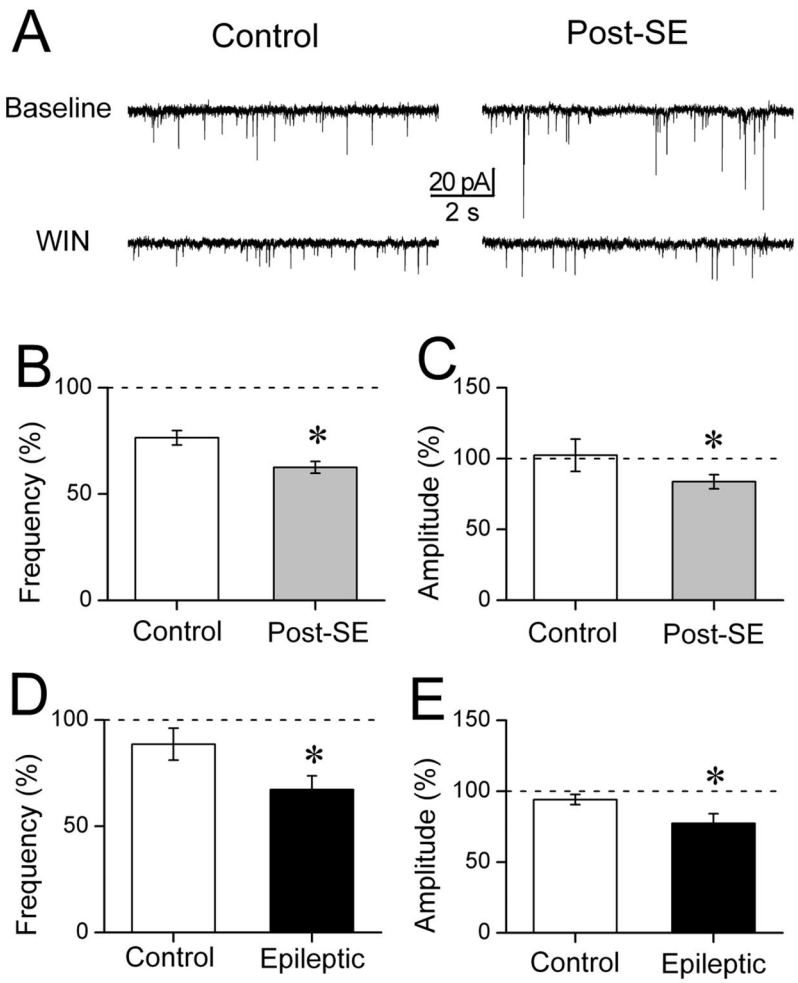

Figure 8. CB_1R-sensitive inhibition of AC-INs is increased in epilepsy

(A): Representative traces show sIPSCs in AC-INs from control (left panel) and one week post-SE (right panel) rats. Note that sIPSC amplitude reduced following bath-application of the CB_1R agonist, WIN-55212 (10 μM, lower traces). (B–C): Summary plots of WIN effect on sIPSCs frequency (B, normalized to baseline) and amplitude (C, normalized to baseline) showed enhanced WIN suppression of sIPSCs in AC-INs after SE (*$p<0.05$, t-test, compared to control). (D–E): Summary plots of WIN effects on sIPSCs frequency (D) and amplitude (E) in epileptic rats. Note that the increase in WIN suppression of sIPSCs observed one week after SE persists in epileptic rats. (*$p<0.05$, t-test, compared to control).